

# Transient Contraction of Muscle Fibers on Photorelease of ATP at Intermediate Concentrations of $\text{Ca}^{2+}$

K. Horiuti, K. Kagawa, and K. Yamada

Department of Physiology, Oita Medical University, Oita 879-55, Japan

**ABSTRACT** We isometrically activated skinned fibers in rigor by flash photolysis of caged ATP at various  $[\text{Ca}^{2+}]$  at  $8^\circ\text{C}$ . On release of ATP, tension initially decreased with the same time course at all  $[\text{Ca}^{2+}]$ . At high  $[\text{Ca}^{2+}]$  ( $\text{pCa} \leq 5.8$ ), tension rose to the steady-state plateau after the brief relaxation. When the  $[\text{Ca}^{2+}]$  was intermediate ( $7.0 \leq \text{pCa} \leq 6.0$ ), tension temporarily overshoot the final steady-state level. The half-time during this tension transient was longer at higher  $[\text{Ca}^{2+}]$ . The transient contractions could be simulated by a simple kinetic model:  $R + \text{ATP} \rightarrow Q$ , and  $X \leftrightarrow Q \leftrightarrow A$ , where  $R$ ,  $X$ , and  $A$  are the rigor, relaxed, and active-tension states, respectively;  $Q$  is a “pre-active” state where tension is very low; and  $\text{Ca}^{2+}$  affects only the  $X$ - $Q$  transition. This scheme was also useful for predicting the tension transients in  $\text{Ca}^{2+}$ - and  $\text{P}_i$ -jump experiments at various  $[\text{Ca}^{2+}]$ . ADP enhanced the  $\text{Ca}^{2+}$  sensitivity of the ATP-induced transient contraction, which was not in the scope of the model.

## INTRODUCTION

The contractile reaction of actin and myosin in vertebrate skeletal muscle is regulated by  $\text{Ca}^{2+}$  ions through the regulatory proteins on actin filaments: troponin and tropomyosin (Ebashi et al., 1969).  $\text{Ca}^{2+}$  binds to troponin, canceling the inhibitory action of tropomyosin on actin. The cross-bridge, i.e., the complex of actin and myosin, is an ATPase and converts the chemical energy of ATP hydrolysis into the mechanical work of muscle contraction.

One of the mysteries of the cross-bridge reaction is the effect of  $\text{Ca}^{2+}$  regulation on its kinetics (Millar and Homsher, 1990; Walker et al., 1992). Under some conditions,  $[\text{Ca}^{2+}]$  seems to affect the cross-bridge transition between the relaxed state and the state of force generation, but does not under other conditions. For example, the rate of tension development after the manipulation of restretch-after-shortening is greatly dependent on  $[\text{Ca}^{2+}]$  (Brenner, 1988), whereas the rate of tension decline on flash photolysis of caged  $\text{P}_i$  is scarcely dependent on  $[\text{Ca}^{2+}]$  (Millar and Homsher, 1990; Walker et al., 1992). In addition, according to the short report by Walker and Moss (1990), the rate of tension generation after photolysis of caged ATP was also independent of  $[\text{Ca}^{2+}]$ .

We have been characterizing the contraction and relaxation that are induced by photolysis of caged ATP in rat psoas fibers and have proposed a model of cross-bridge kinetics based on our results (Horiuti et al., 1992b; 1994). It seemed to us that this model solves the above kinetic problem with the effect of  $[\text{Ca}^{2+}]$ . Thus, we examined in this study the  $\text{Ca}^{2+}$  dependence of the ATP-induced contraction. The contraction at intermediate  $[\text{Ca}^{2+}]$  had a transient peak before reaching the low steady level, which was consistent with the model. We quantitatively defined the model using the results with

caged ATP, and used it to simulate the tension transients in experiments with caged  $\text{Ca}^{2+}$  and  $\text{P}_i$ .

## MATERIALS AND METHODS

The materials and setups were the same as previously described (Horiuti et al., 1992a, b). Briefly, a segment (0.1 mm thick, 1.5 mm long) of a skinned muscle fiber from rat psoas was tied to a force transducer (AE 801, SensoNor, Norway) at one end and to a compound piezo actuator (P835.10 in series with P841.60, Physik Instrumente, Germany) at the other end. The fiber tension was monitored with the transducer using a signal conditioner (CDV-230C, Kyowa Electronic Instruments, Japan). To monitor 500-Hz stiffness of the fiber, we applied a sinusoidal length oscillation (3  $\mu\text{m}$  peak-to-peak) to the fiber through the actuator and demodulated the resultant tension oscillation using a lock-in amplifier (5610B, NF Electronic Instruments, Japan). The in-phase- and quadrature stiffness in this paper refer to  $A \cdot \cos(\theta)$  and  $A \cdot \sin(\theta)$ , where  $[A, \theta]$  is the [amplitude, phase-shift] of the tension oscillation. The tension and stiffness signals were digitized for storage after low-pass-filtering at 200 Hz.

We put the fiber in the rigor state by washing with an ATP-free solution and then introduced caged ATP (see below for the composition of the photolysis solution). After allowing time for the solution to diffuse into the fiber (30 s), we applied an ultraviolet flash from a xenon lamp (LH-HF with SA-200E, Eagle Corporation, Japan) to the fiber at  $7$ – $9^\circ\text{C}$ . 22–25% of the caged ATP could be photolyzed with a single flash to induce contraction or relaxation of the fiber. 5 s before photolysis, we stretched the fiber by 14  $\mu\text{m}$ , using the piezo actuator, to increase the rigor tension.

The caged ATP solution for photolysis contained (mM): 3.8 caged ATP, 10  $\text{MgCl}_2$ ,  $x$   $\text{CaCl}_2$ , 10 EGTA, 20 PIPES, 10 dithiothreitol, and an appropriate amount of KCl for the ionic strength of 0.20 M, pH being adjusted to 7.0 with KOH at room temperature. The concentration of  $\text{CaCl}_2$  ( $x$ ) was 0 mM to induce complete relaxation ( $\text{pCa} > 8$ ; solution G) and 10 mM to induce a maximum contraction ( $\text{pCa} \approx 4.5$ ). We adopted  $10^{6.264} \text{ M}^{-1}$  as the apparent stability constant of CaEGTA under our experimental conditions. Thus,  $x = 3.16$  for  $\text{pCa}$  6.6, 4.23 for 6.4, 5.37 for 6.2, 6.48 for 6.0, and 7.44 for 5.8. We added 12 mM  $\text{P}_i$  (orthophosphate, K salt) in the  $\text{Ca}^{2+}$ -free solution, referred to as G, for complete suppression of the contractile activity that usually remained even with no added  $\text{Ca}^{2+}$  (see Fig. 4 of Horiuti et al., 1992a). If a significant contraction had existed in the  $\text{Ca}^{2+}$ -free record, a part of contraction in each  $\text{Ca}^{2+}$  record had been canceled in the subtraction analysis described in Results.

Caged ATP was purchased from Dojindo Lab (Japan). The batch used in this study was reported to contain a relatively high concentration of ATP (0.026% or 1.2  $\mu\text{M}$  ATP in the photolysis solution) compared with that used in our previous study ( $<0.008\%$ ; Horiuti et al., 1992b). This contaminating ATP should have been converted into ADP in muscle, and this ADP might

Received for publication 23 November 1993 and in final form 20 June 1994.

Address reprint requests to Dr K. Horiuti, Department of Physiology, Oita Medical University, Hasama, Oita 879-55, Japan. Fax: 81-975-49-4244.

© 1994 by the Biophysical Society

0006-3495/94/11/1925/08 \$2.00

have affected our results without added ADP (Thirlwell et al., 1993). The effect of added ADP, however, was significant at 20  $\mu\text{M}$  and increased about 2.5 times at 60  $\mu\text{M}$ . The magnitude of ADP effect was evaluated by the size of the rapid tension development on ATP release in solution G, the details of which will be presented in a subsequent paper.

In Fig. 1 is shown the tension transient obtained following photorelease of ATP at pCa 6.1, which has been already corrected for the initial rigor degradation by the subtraction method (see Results). The half-time of tension rise was measured as follows (Fig. 1, *bottom*): We fitted a line on the steepest part of the rising phase, and determined its intersection point (d) on the baseline (b). Next, we found that point (r) on the curve which was on the level halfway up from the baseline (b) to the peak level (p). The half-time was defined as the time from d to r. When the  $[\text{Ca}^{2+}]$  was high, tension increased monotonically. In this case, we took the plateau as the level p. The plateau had a slow creep because we used no ATP-regenerating system in this work. Tension slowly increased with the gradual consumption of ATP and accumulation of ADP (Horiuti et al., 1992a). The initial plateau level was defined as the level reached at 0.75 s after the photorelease of ATP.

To determine the half-time for tension to fall from the peak (Fig. 1, *top*), a line was fitted at the steepest part of the tension fall and this line was extrapolated back to the peak level (p) to determine the crossing point (e). We then marked that point (f) on the curve which was halfway down from the peak level (p) to the steady-state level (s). The falling half-time was defined as the time from e to f. The steady-state level was defined as the level measured 8 s after ATP release.

### Collection and presentation of the data

The main data shown in this paper were taken from four types experiments. In two of the four, we examined the effect of  $[\text{Ca}^{2+}]$  in the absence of ADP. In one of the two, the contraction records were taken at pCa 4.5, 5.8, and 6.0 and in solution G (EGTA +  $\text{P}_i$ ), and in the other at pCa 4.5, 6.1, 6.2, 6.4, and 6.6, and in solution G. We performed the other two types of experiments to examine the effect of ADP, one at pCa 6.6 and the other at pCa 6.1. In both experiments, the control records with and without ADP were also taken at pCa 4.5 and in solution G. The G records were necessary for the subtraction analysis (see Results).

We repeated each experiment using five different muscle fibers and changed the order of the experimental trials. The records in each experiment were averaged over the five trials, and the quantitative analysis was made only on the averaged records. The tracings in Figs. 1–3 and 6 are the averaged ones, and values quoted in the text and Figs. 4, 5, and 7 were obtained on the averaged records. However, unless otherwise stated, the validity of any qualitative statements in Results was verified with each of the five data

sets. If the same result occurred at each of the five data sets only by chance with random errors or noise, its probability ( $P$ ) was  $(1/2)^5$  ( $= 3\%$ ).

### RESULTS

We activated the rigor fibers by photorelease of 1 mM ATP at various  $[\text{Ca}^{2+}]$ . In Fig. 2 are some examples of tension records. In the absence of  $\text{Ca}^{2+}$  (G), the rigor tension on ATP release dropped rapidly to the relaxing level. The half-time of relaxation was approximately 28 ms. This estimate of the half-time included the 7 ms delay, which could be due to the finite rate of ATP release ( $\approx 40 \text{ s}^{-1}$  under our conditions; Goldman et al., 1984a). Even in the presence of saturating  $\text{Ca}^{2+}$  (pCa 4.5), tension initially declined as in its absence, but later started rising to reach the steady-state plateau. These observations were consistent with the previous ones from rabbit and rat psoas muscles (Goldman et al., 1984a, b; Horiuti et al., 1992b).

When we reduced  $[\text{Ca}^{2+}]$  to intermediate concentrations (e.g., pCa 6.1 and 6.4), the contraction after the initial rigor degradation became biphasic exhibiting a peak before reaching a lower steady-state level. At pCa 6.4, although the steady-state tension was minimal, the peak was as high as 38% of the maximum tension at pCa 4.5. Transient contractions at  $7.0 \leq \text{pCa} \leq 6.0$  were confirmed in two similar experiments, each conducted with 3 fibers. (These data were not included in the analysis in this paper.) The transient contraction at intermediate  $[\text{Ca}^{2+}]$  in rabbit psoas has been also reported briefly by Goldman and Hibberd (1983).

The records of 500-Hz stiffness at pCa 6.4 are superimposed on the tension record in Fig. 3 (*bottom*), where the two

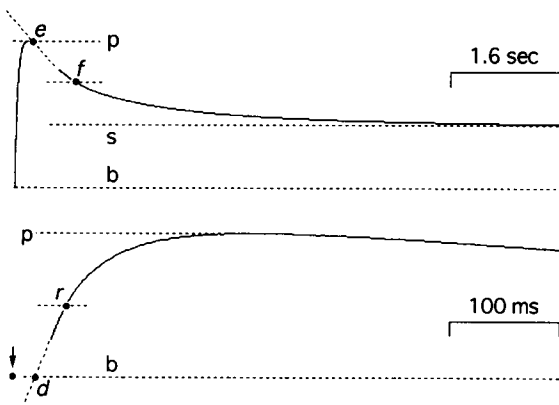


FIGURE 1 Illustration of the method used to measure the half-times for rising phase (*bottom*) and falling phase (*top*) of tension. These are the same records shown on different time bases. The left-most arrow in the lower panel indicates the moment of ATP release. For clarity, some parts of the tracings are erased. See text for detail.

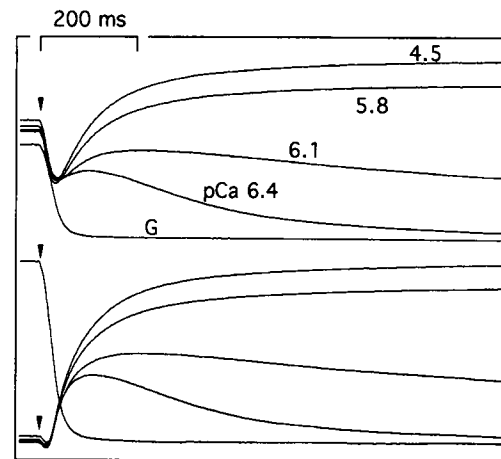


FIGURE 2 Tension transients on photorelease of ATP at various  $[\text{Ca}^{2+}]$ . The record G was obtained in the  $\text{Ca}^{2+}$ -free solution with  $\text{P}_i$  (solution G). The tracings in the upper panel are the original records. In the lower panel, the records with  $\text{Ca}^{2+}$  were corrected for the initial falling phase by subtraction of the appropriately scaled G record. Note that the record G is shown also in the lower panel to be compared with the corrected records. 0.97 mM ATP was released at the moment indicated with the arrow heads. The two records at pCa 4.5 and 5.8 and the other three records were obtained in two separate experiments. The records obtained at low  $[\text{Ca}^{2+}]$  are scaled so that the pCa 4.5 tracing in the same experiment (not shown) would have the same height as the one in this figure.

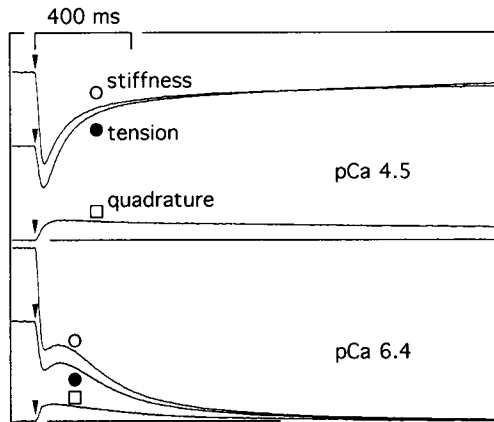


FIGURE 3 The records of tension (●), in-phase stiffness (○), and quadrature stiffness (□) at 500 Hz. The upper records were obtained at pCa 4.5 and the lower ones at pCa 6.4. Note that the tracings are scaled so that the tension and in-phase stiffness have the same height at 1 s after ATP release at pCa 4.5. The two sets of records were obtained from the same fibers.

signals are normalized to their sizes in the steady state at pCa 4.5 (*top*). As shown in Fig. 3, the ratio of tension to stiffness at the peak of the transient contraction at pCa 6.4 was 24% lower ( $P = 3\%$ ) than that during the maximum steady contraction at pCa 4.5. At pCa 6.1, the low tension/stiffness ratio was the case for a long time ( $>20$  s) after the peak (not shown). The low tension/stiffness ratio was also observed in the presence of an ATP-regenerating system in the photolysis solution (10 mM creatine phosphate plus 0.5 mg/ml creatine phosphokinase) at pCa 6.0 with three muscle fibers.

This low tension/stiffness could not be attributed to the lengthening of the end-compliance, because this happened at the tension peak. The high stiffness at low tension was also in the opposite direction to what was expected from the non-linear end-compliance (Goldman et al., 1984a). Because this tension-stiffness dissociation could last for quite a long time, it could not be caused by the rigor cross-bridges remaining after the release of ATP. From the time courses of tension and stiffness (Figs. 2 and 3), one would expect the rigor bridges to have disappeared within about 100 ms. Because the tension-stiffness dissociation could be seen also in the presence of the ATP-regenerating system, it was not likely caused by formation of rigor bridges during the contraction.

The time course of the signal of quadrature stiffness is also shown in Fig. 3. Its peak during the transient contraction (pCa 6.4) was 20% smaller than the peak during the maximum contraction (pCa 4.5). The transient peak of the in-phase stiffness (pCa 6.4) was about 50% lower than the maximum plateau (pCa 4.5). This indicated that during the transient contraction the quadrature stiffness was disproportionately large compared with the in-phase stiffness. This was true with all five records at pCa 6.4, so that it was statistically significant ( $P = 3\%$ ). The dissociation of quadrature stiffness from in-phase stiffness was observed also at pCa 6.1 (not shown).

To analyze the effects of  $[\text{Ca}^{2+}]$ , we corrected each tension record for the initial  $\text{Ca}^{2+}$ -independent rigor degradation

(Fig. 2, *bottom*) by subtracting the relaxing  $G$  record (Horiuti et al., 1992b). It is notable that the initial slope of the corrected records was quite constant and independent of  $[\text{Ca}^{2+}]$ . This is illustrated in a different manner in Fig. 4. The peak size and the half-time to peak are proportional, indicating the constant initial slope ( $\approx 1/2 \times \text{peak size}/\text{half-time}$ ).

To characterize the corrected  $\text{Ca}^{2+}$  records, we measured four quantities on each records as shown in Fig. 5: the peak tension, the steady level of tension, the half-time for rising phase to the peak (or steady plateau), and the half-time for falling phase from the peak. (1) The relation of the steady-state tension with the  $[\text{Ca}^{2+}]$  was quite steep. (2) The relation between the peak height and  $[\text{Ca}^{2+}]$ , however, tailed toward the low  $\text{Ca}^{2+}$  range. (3) The half-time for the tension rise was longer at higher  $[\text{Ca}^{2+}]$ . (4) The  $\text{Ca}^{2+}$  dependence of the falling half-time appeared to be bell-shaped, having a peak at around pCa 6.1. Only 3 out of the 5 fibers showed falling phases at pCa 6.0, so that the bell shape was not statistically significant.

ADP has been known to increase  $\text{Ca}^{2+}$  sensitivity of the steady-state contraction (Hoar et al., 1987). Thus, we examined the effects of ADP on the transient kinetics of the ATP-induced contraction. As shown in Fig. 6, the addition of 0.6 mM ADP in the photolysis solution delayed and slowed the ATP-induced initial rigor degradation. This was most clear in the absence of  $\text{Ca}^{2+}$  (Fig. 6, *G*). This effect was consistent with the results in the previous studies (Dantzig et al., 1991; Horiuti et al., 1993) and has been assumed to be from competition of ADP with ATP and from some mechanism not fully understood.

Even in the presence of ADP,  $\text{Ca}^{2+}$  did not change the initial time courses of tension (Fig. 6) and stiffness (not shown), so that we could analyze the  $\text{Ca}^{2+}$ -sensitive contraction in the presence of ADP by the subtraction method used in the experiments described above. The results of this analysis at pCa 6.4, 6.1, and 4.5 are plotted in Figs. 4 and 5, where the crosses represent the data in the presence of ADP and the squares represent the control data without added ADP in the same experiments.

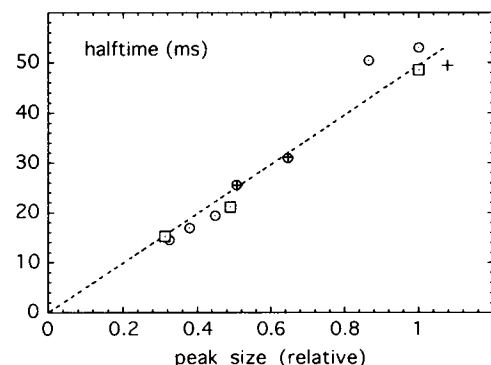


FIGURE 4 Relation of the peak size and the half-time for the rising phase of tension. The circles (○) represent the data obtained in the experiments shown in Fig. 2. The crosses (+) represent the data taken in other experiments, where the photolysis solution contained 0.63 mM ADP (Fig. 6). The squares (□) indicate the control data in the ADP experiments.

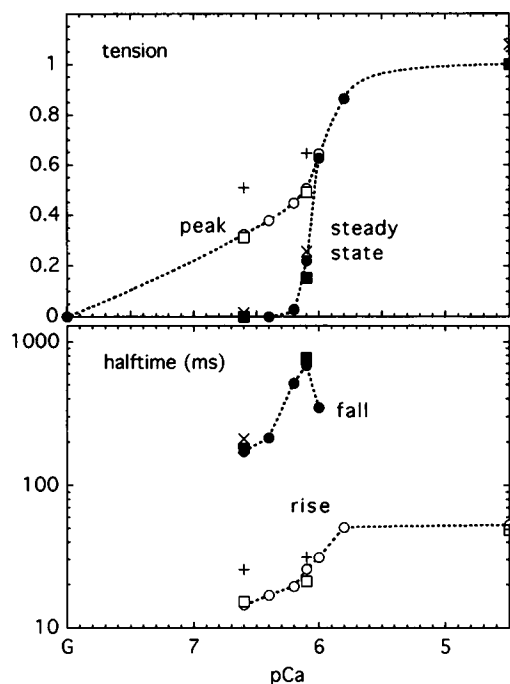


FIGURE 5 Summary of the tension transients at various  $[Ca^{2+}]$ . The upper panel shows the peak and the steady-state tension, and the lower panel shows the half-times for the rising and falling phases of tension. The circles (○, ●) represent the data in the absence of ADP, the crosses (+, ×) in the presence of 0.63 mM ADP, and the squares (□, ■) the control data in the ADP experiments. Note that one cross (×) is hidden by the filled square at pCa 6.1 in the lower plot.

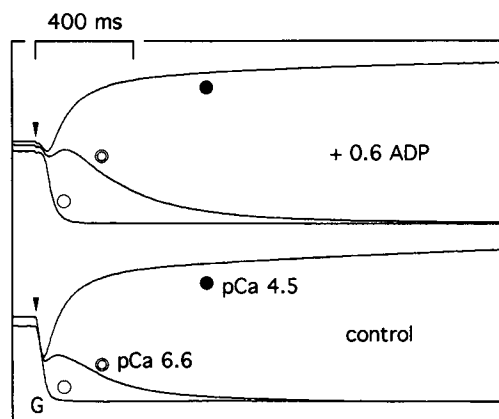


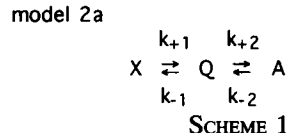
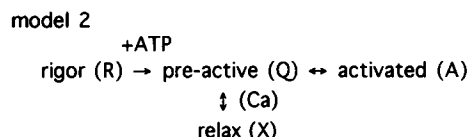
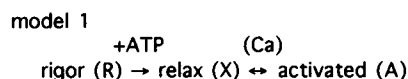
FIGURE 6 Tension records on release of 0.84 mM ATP, in the presence (top) and absence (bottom) of 0.63 mM ADP. The records labeled with ● and ○ were obtained at pCa 4.5 and 6.6, respectively, and that labeled with ○ in solution G (EGTA +  $P_i$ ).

ADP increased the steady-state tension at pCa 6.1 by 68%, but the increase was only 8% at pCa 4.5 (Fig. 5). Thus, the ADP effect at intermediate  $[Ca^{2+}]$  appeared to be mainly from the action of ADP that increases  $Ca^{2+}$  sensitivity of the contractile system. Although ADP did not significantly change the initial speed of the tension rise (Fig. 4), it greatly increased the peak size (by 32 and 62% at pCa 6.1 and 6.4, respectively; Figs. 5 and 6). A similar effect could be seen

when we reduced amount of photoreleased ATP by a factor of 4 in the absence of added ADP (three fibers; not shown).

## DISCUSSION

Even at supramaximal  $[Ca^{2+}]$ , muscle fibers initially relax before contraction on release of ATP (Goldman et al., 1984a). This phenomenon has been described adequately with a sequential reaction model (model 1) in Scheme 1. The cross-bridge state immediately after the binding of ATP is the relaxed state (X), and the transition to the force-generating or activated state (A) is controlled by  $Ca^{2+}$ . However, it is difficult to explain the transient contractions observed at intermediate  $[Ca^{2+}]$ . After binding of ATP, the reaction is a two-state transition between X and A. Therefore, the time course of A is always monotonic regardless of the rate constants for the transition.



Transient contractions on release of ATP also appear even in the absence of  $Ca^{2+}$  when the amount of released ATP is low (Goldman et al., 1984b). Even at 0.3 mM ATP this contraction is evident, and at  $\approx 0.13$  mM ATP it reaches the maximum magnitude, which is  $\approx 40\%$  of the maximum contraction with saturating  $Ca^{2+}$  and ATP (rat psoas at 16°C; Sakoda and Horiuti, 1992). The low ATP contraction seems to be essentially the same as the transient contraction at intermediate  $[Ca^{2+}]$  with saturating ATP ( $\approx 1$  mM). Lowering the ATP concentration potentiates the effect of ADP on the transient. Indeed, the transient contractions at intermediate  $[Ca^{2+}]$  were enhanced by reductions in the photoreleased ATP similar to the addition of ADP (this study). Goldman and colleagues (Goldman et al., 1984a, b) explained the low ATP contraction in the absence of  $Ca^{2+}$  using model 1 by permitting interaction among the cross-bridges. A transient contraction can be simulated by model 1 if one postulates that, even without  $Ca^{2+}$ , one of the two heads of the myosin molecule enters state A from X when the other head is not in state X (Goldman et al., 1984a).

The above bridge-to-bridge interaction was assumed to be a result of the protein cooperativity in muscle. Not only the regulatory proteins affect cross-bridge activity but, also, the

cross-bridges in turn influence the state of regulatory proteins. The  $\text{Ca}^{2+}$ -binding of the regulatory proteins is enhanced by attachment of the cross-bridges (Bremel and Weber, 1972; Fuchs, 1977). Therefore, a cross-bridge may interact with other cross-bridges through the regulatory proteins. In fact, even in the absence of  $\text{Ca}^{2+}$ , muscle generates tension with a high ATPase activity when [ATP] is low so that the cross-bridges favor the attached state (Rueben et al., 1971; Bremel and Weber, 1972). Some form of the interactions among the cross-bridges and regulatory proteins might be the cause of the transient contraction on release of ATP at intermediate  $[\text{Ca}^{2+}]$ .

If we could quantitatively modify model 1 incorporating various types of cooperative interactions, it would explain the transient contraction at intermediate  $[\text{Ca}^{2+}]$ , but such a model would be very complex. Instead of adding cooperativity to model 1, we attempted to describe the transient contraction using a simple kinetic model proposed in our previous studies with caged ATP (Horiuti et al., 1992b, 1994). Although this simple model might be just a phenomenological way of describing cooperativity, it has the added advantage of simulating mechanical transients other than those observed in the caged ATP experiments.

### The ATP-induced transient contraction in the model

Our idea is shown as model 2 in Scheme 1. The intermediate state between the rigor state ( $R$ ) and the tension-generating state ( $A$ ) is not the relaxed state ( $X$ ) but a "pre-active" state ( $Q$ ), and  $\text{Ca}^{2+}$  regulates the branch from  $Q$  to  $X$ .  $Q$  is similar to  $X$  in that it bears no force and little (in-phase) stiffness (Horiuti et al., 1992b).  $Q$  is, however, similar to  $A$  in that it bears high quadrature stiffness at high frequencies (Horiuti et al., 1992b) and the high intensity of the equatorial  $[1,1]$  reflection of x-ray (Horiuti et al., 1994). As discussed previously (Horiuti et al., 1992b, 1994), state  $Q$  seems to be similar to, but not the same as, the "weak binding state" (Brenner et al., 1982) at low ionic strengths.

In our previous scheme (Horiuti et al., 1992b), another state (" $Q+P$ ") was also introduced between  $Q$  and  $A$ . This was because in ATP-induced contractions from rigor the high frequency quadrature stiffness appeared to rise earlier than the in-phase component of stiffness, and the latter rose still earlier than tension. In the present study, similar time courses were observed for stiffness and tension at the high  $[\text{Ca}^{2+}]$  (Fig. 3, *top*; detailed analysis not shown). In addition, at intermediate  $[\text{Ca}^{2+}]$  (Fig. 3, *bottom*) it was found that [tension] < [in-phase stiffness] < [quadrature stiffness] at the peak of the transient contraction when the three signals were compared with those measured during the steady phase of contractions at high  $[\text{Ca}^{2+}]$ . This discrepancy among the peak sizes of tension and stiffness was probably because the muscle fiber was almost maximally activated at the onset of the transient but was deactivated later by some processes.

In this paper, we do not introduce " $Q+P$ " in the model to keep the model general and choose to discuss only the relationship between the  $[\text{Ca}^{2+}]$  and the tension time course. In

the following argument, the essential property of  $Q$  is only that this state of the cross-bridges bear little force and (in-phase) stiffness.

Our model provides a qualitative explanation for the transient contraction as follows. After the rapid binding of ATP, the reaction starting from  $Q$  is a transition among the three states as in model 2a (Scheme 1). With an appropriate set of values for the four rate constants, cross-bridges can be initially in the activated state ( $A$ ) and later move back to the relaxed state ( $X$ ). The initial speed of increase in  $A$  ( $dA/dt|_{t=0}$ ) is  $k_{+2}$ , so that it is independent of  $[\text{Ca}^{2+}]$  in the model, like in the experimental results (Fig. 4).

The time course of  $A$  in model 2a is generally expressed as the sum of two fading exponentials with an offset (Dawes and Davidson, 1972):

$$A(t) = (-A_1) \cdot \exp(-t/\tau_1) + (-A_2) \cdot \exp(-t/\tau_2) + A_\infty \quad (1)$$

where the time constants ( $\tau_1, \tau_2$ ) and the offset ( $A_\infty$ ) are functions of only the rate constants ( $k_{+1}, k_{-1}, k_{+2}, k_{-2}$ ), whereas the amplitudes ( $A_1, A_2$ ) depend on the initial condition as well. We defined the rate constants using the experimental data (Fig. 7; Appendix), assuming that only  $k_{+1}$  and  $k_{-1}$  are  $\text{Ca}^{2+}$ -dependent. Using the model, we calculated  $A(t)$  at various  $[\text{Ca}^{2+}]$ , setting  $Q = 1$  at  $t = 0$ , and the result is shown in Fig. 8 A. These data should be compared with the experimental data in the lower panel of Fig. 2.

The  $\text{Ca}^{2+}$  dependence of  $A_{\text{peak}}$  (peak size of  $A$ ),  $A_\infty$ ,  $\tau_1$ , and  $\tau_2$  is illustrated in Fig. 8 B and should be compared with Fig. 5. In the upper plot of Fig. 8 B, the maximum  $A_\infty$  is 0.6 because  $K_2 (=k_{+2}/k_{-2})$  has been set at 0.6. The experimentally determined  $\text{Ca}^{2+}$  dependence of  $A_{\text{peak}}$  and  $A_\infty$  are reasonably reproduced in the model, because we directly used these data for the construction of the model (Appendix).

We find that the  $\text{Ca}^{2+}$ -dependent  $\tau_1$  and  $\tau_2$  also mimic the experimentally obtained half-times (Fig. 5, *bottom*). In the model, when  $\text{pCa} > 5.86$ ,  $A(t)$  has a peak (Fig. 8) and  $A_2 > 0 > A_1$ , so that  $\tau_2$  is the time constant for the rising phase and  $\tau_1$  is for the falling phase. When  $\text{pCa} < 5.85$ , both  $A_1$  and  $A_2$  are positive and  $A(t)$  has no peak (Fig. 8). When  $\text{pCa} < 5.68$ ,

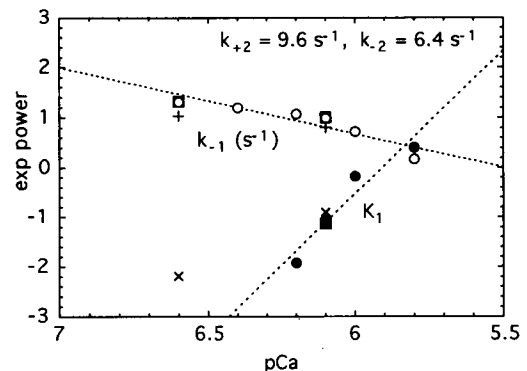


FIGURE 7 Estimation of  $k_{-1}$  ( $\circ, \square, +$ ) and  $K_1 (=k_{+1}/k_{-1}; \bullet, \blacksquare, \times)$ . The symbols are as in Fig. 5. Note that this is a double-logarithmic plot. The broken lines are the regression lines fitted to the data without added ADP ( $\circ, \bullet$ ).

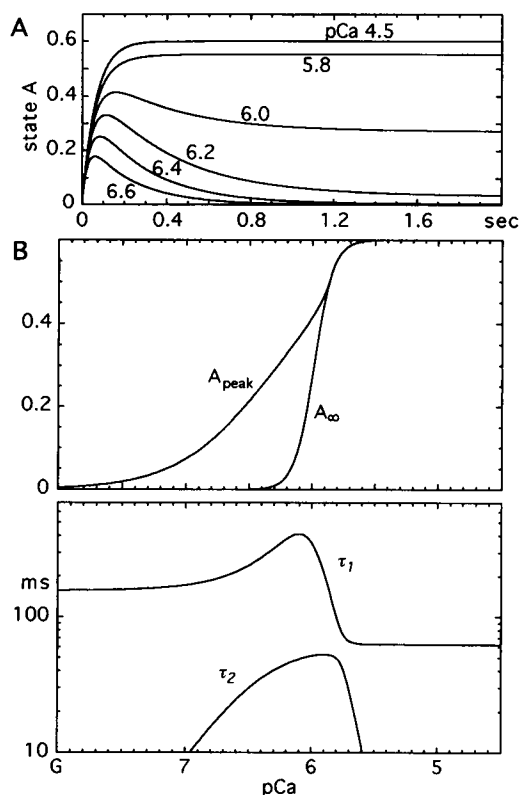


FIGURE 8 (A) Time course of state A from model 2a with  $Q = 1$  at  $t=0$ . The labels represent the pCa values. (B) Summary of the time courses. Upper plot shows the  $\text{Ca}^{2+}$  dependence of the peak height ( $A_{\text{peak}}$ ) and the steady-state level ( $A_{\infty}$ ), and the lower plot shows the  $\text{Ca}^{2+}$  dependence of the two time constants ( $\tau_1$ ,  $\tau_2$ ).  $A_{\text{peak}}$  was numerically obtained by scanning  $t$  in  $A(t)$  from 0 through 2 s with 2-ms resolution.

$A_2$  is negligibly small ( $A_2/A_1 < 5\%$ ; not shown) so that  $\tau_1$  is the time constant for the monotonic rising of  $A(t)$ .

#### Effect of ADP on the caged ATP transient

We found that ADP increases the  $\text{Ca}^{2+}$  sensitivity of the transient contraction at intermediate  $[\text{Ca}^{2+}]$  (see Figs. 5 and 6). The idea of  $\text{Ca}^{2+}$  sensitization by ADP has been proposed (Hoar et al., 1987) from the ADP effect on the steady-state tension at various  $[\text{Ca}^{2+}]$ . Our results are the first data from transient kinetic studies to show that this idea is valid (Figs. 4 and 5).

An important point is that this  $\text{Ca}^{2+}$ -sensitizing effect of ADP cannot be explained by simple competition of ADP with ATP in our model. In model 2, even if we reduce the rate of  $R$ -to- $Q$  transition, the transient contraction does not increase in size. In such a case, the peak actually becomes smaller than the control because of the more asynchronous initiation of the contraction. As mentioned earlier, a reduction of the amount of photoreleased ATP increases the  $\text{Ca}^{2+}$  sensitivity of the contraction and induces a transient contraction even without  $\text{Ca}^{2+}$ . However, again, this cannot be explained by the slow  $R$ -to- $Q$  transition in our model. To explain the ADP/ATP effect, we must assume that the nucle-

otides somehow affect the  $X$ - $Q$  transition like  $\text{Ca}^{2+}$ . This effect could be caused by a type of protein cooperativity.

#### Application of the model to other types of experiments

We applied the model with state  $Q$  (model 2a) to the tension transients in the caged  $\text{Ca}^{2+}$  and caged  $\text{P}_i$  experiments (see below for references) and found the model is also useful for interpreting such transients. The three sets of tracings in Fig. 9 are  $A(t)$ s calculated in model 2a with different initial conditions at the same five  $[\text{Ca}^{2+}]$ . In the lowest panel, the reactions start from  $Q$  with the release of ATP like in Fig. 8.

The middle panel of Fig. 9 illustrates a simulation using model 2a of the tension development at various  $[\text{Ca}^{2+}]$  in the caged  $\text{Ca}^{2+}$  experiments (Goldman and Kaplan, 1988; Ashley et al., 1991) and the conventional  $\text{Ca}^{2+}$ -jump experiments (Moisescu, 1976; Griffiths et al., 1979). The initial condition,  $X = 1$  at  $t = 0$ , results in  $\tau_1$  and  $\tau_2$  being time constants for the main rising phase and the initial lag phase, respectively. It should be noted that the rate ( $k_w$ ) of tension development at various  $[\text{Ca}^{2+}]$  in the stretch-after-shortening experiments (Brenner, 1988) has been assumed (Millar and Homsher, 1990; Walker et al., 1992) to be essentially the same as that ( $k_{\text{Ca}}$ ) in the experiments with jumps in  $[\text{Ca}^{2+}]$ .

As in Fig. 9 (middle), the absolute speed and the rate constant ( $k_{\text{Ca}}$  or  $k_w$ ) of tension development from the relaxed state ( $X$ ) are remarkably dependent on  $[\text{Ca}^{2+}]$  in the model. This property is from the  $\text{Ca}^{2+}$ -dependent  $X$ - $Q$  transition and

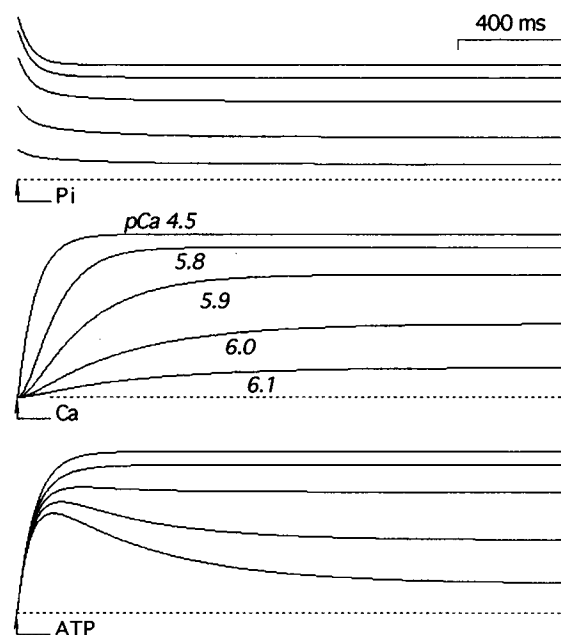


FIGURE 9 Simulation by model 2a of the tension transient in the caged  $\text{P}_i$  (top), caged  $\text{Ca}^{2+}$  (middle), and caged ATP (bottom) experiments. In all of the panels, the tracings are the transients at the same five pCAs, although they are labeled only in the middle panel. We obtained the data numerically by a method of sequential linear approximation, where the sum of fluxes was kept less than 1% of the total mass at each short time step.

is consistent at least qualitatively with the experimental observations of  $k_{\text{Ca}}$  and  $k_{\text{tr}}$  (the same references as above). The different  $\text{Ca}^{2+}$  dependence of  $k_{\text{ATP}}$  and  $k_{\text{Ca}}/k_{\text{tr}}$  has been vaguely explained with the idea of cross-bridge cooperativity (Millar and Homsher, 1990). ( $k_{\text{ATP}}$  is the rate of tension rise in the caged ATP experiment.)

The top panel of Fig. 9 is simulation of the caged  $\text{P}_i$  experiments. According to the previous studies (Hibberd et al., 1985; Millar and Homsher, 1990; Walker et al., 1992), addition of  $\text{P}_i$  essentially accelerates the backward rate of the transition for force generation. Thus, we initially put model 2a in the steady state at various  $[\text{Ca}^{2+}]$ , and then increase  $k_{-2}$  by a factor of two at  $t = 0$ . On elevation of  $k_{-2}$ , the population in A decreases in two phases with short  $\tau_2$  and long  $\tau_1$ .

As has been discussed by Millar and Homsher (1990) and Walker et al. (1992), if we simply adopt model 1, the rate of tension decline in the caged  $\text{P}_i$  experiment ( $k_{\text{pi}}$ ) must be the same as  $k_{\text{tr}}$  at any  $[\text{Ca}^{2+}]$ . Instead, their experimental results showed that (1) the  $\text{Ca}^{2+}$  dependence of  $k_{\text{pi}}$  was smaller than that of  $k_{\text{tr}}$  and (2)  $k_{\text{pi}}$  was larger than  $k_{\text{tr}}$  (2a) even at  $[\text{Ca}^{2+}]$  sufficiently high for maximum activation. Furthermore, (3) the tension transient was complex, consisting of a rapid tension decline with  $k_{\text{pi}}$  and another gradual decline with  $k_{\text{slow}}$ . Although (4) the relative amplitude of the slow phase greatly increased as decreasing  $[\text{Ca}^{2+}]$ , (4a) its rate ( $k_{\text{slow}}$ ) was independent of the  $[\text{Ca}^{2+}]$  (Walker et al., 1992).

As is shown in Fig. 9 (top), many of the above features (1–4) are reproduced in the model. However, some features are not reproduced: (2a) at pCa 4.5 (and a given  $[\text{P}_i]$ ), the model predicts that  $k_{\text{pi}} = k_{\text{tr}} = k_{\text{ATP}} (=1/\tau_1)$ . Experimentally,  $k_{\text{tr}}$  has been reported to be approximately the same as  $k_{\text{ATP}}$  (Burton et al., 1989), but  $k_{\text{pi}}$  appears twofold larger than  $k_{\text{tr}}$  (Millar and Homsher, 1990; Walker et al., 1992). It will be important in future studies to examine the three rates under the same conditions. (4a) At low  $[\text{Ca}^{2+}]$ ,  $k_{\text{slow}} (=1/\tau_1)$  in the model is  $\text{Ca}^{2+}$ -dependent, contrary to the experimental result (Walker et al., 1992). It should be noted that the actual caged  $\text{P}_i$  transients were not simply double-exponential and that the two exponential phases of tension decline were intervened with another phase of tension increase. Such a pause is not simulated in the present model.

This study was supported by grants from the Ministry of Education, Science and Culture (Japan), from CIBA-GEIGY Foundation (Japan) for Promotion of Sciences, and from TERUMO Life Science Foundation.

## APPENDIX

In Eq. 1,  $\tau_1$  and  $\tau_2$  are the two roots of the following characteristic equation:  $(1/\tau)^2 - \alpha \cdot (1/\tau) + \beta = 0$ , where  $\alpha = k_{+1} + k_{-1} + k_{+2} + k_{-2}$  and  $\beta = k_{+1}k_{+2} + k_{-2}k_{-1} + k_{+1}k_{-2}$ . When we put the initial condition that  $X = 0$ ,  $Q = 1$ ,  $A = 0$ , and  $dA/dt = k_{+2}$  at  $t = 0$ ,  $A_{\infty} (=A_1 + A_2) = k_{+1}k_{+2}/\beta$ ,  $A_1 = (k_{+2} - A_{\infty}/\tau_2)/(1/\tau_1 - 1/\tau_2)$ , and  $A_2 = (k_{+2} - A_{\infty}/\tau_1)/(1/\tau_2 - 1/\tau_1)$ . Although ( $A_1$ ,  $\tau_1$ ) and ( $A_2$ ,  $\tau_2$ ) are interchangeable, we assign them so as  $\tau_1 > \tau_2$ .

We first estimated the  $\text{Ca}^{2+}$ -independent  $k_{+2}$  and  $k_{-2}$  from the time course of the maximum contraction at pCa 4.5. The basis for this estimation was an additional, plausible assumption that the equilibrium between X and Q greatly favors Q at such a high  $[\text{Ca}^{2+}]$ . In this case, the reaction is a simple

two-state transition between Q and A, so that the rate constant for accumulation of A is equal to  $[k_{+2} + k_{-2}]$ . The half-time of the tension rise at pCa 4.5 was about 50 ms (Fig. 5), the corresponding rate constant being  $14 \text{ s}^{-1}$ . The rate constant estimated directly from the raw tension records by fitting a double-exponential function with a delay (Goldman et al., 1984a; Horiuti et al., 1992a) was approximately  $16 \text{ s}^{-1}$ .

We took 9.6 and  $6.4 \text{ s}^{-1}$  for  $k_{+2}$  and  $k_{-2}$ , respectively, because  $k_{+2}:k_{-2}$  ( $\equiv K_2$ ) seemed to be about 3:2 under our conditions. The reason for the ratio was that the magnitude of (in-phase) stiffness at the maximum contraction was  $62 \pm 6\%$  (SD,  $n = 14$ ) of that at the rigor state induced at pCa 4.5 (K. Kagawa, unpublished observations; see Fig. 2 of Horiuti et al. (1993) for the method).

We then defined the  $\text{Ca}^{2+}$ -dependent  $k_{+1}$  and  $k_{-1}$ . The equilibrium constant  $K_1$  ( $\equiv k_{+1}/k_{-1}$ ) determines the amount of A at  $t = \infty$  in the model:  $A_{\infty} = K_1 K_2 / (1 + K_1 + K_1 K_2)$ . Therefore, we could estimate  $K_1$  at intermediate  $[\text{Ca}^{2+}]$  from the observed size of steady-state tension. For estimation of  $k_{-1}$ , we used the following expression:  $A_{\text{peak}} \approx k_{+2}/(k_{-1} + k_{+2})$ , which we found with small  $k_{+1}$ . By using the observed size of tension peak, we could thus approximate  $k_{-1}$  at low  $[\text{Ca}^{2+}]$ . The estimated  $K_1$  and  $k_{-1}$  are illustrated in the double-logarithmic plot in Fig. 7 (circles and squares). We took the regression lines in this plot as the  $\text{Ca}^{2+}$  dependence of the two variables:  $\log[k_{-1}(\text{s}^{-1})] = -7.31 + 1.33 \text{ pCa}$ , and  $\log[K_1] = 33.9 - 5.73 \text{ pCa}$ .

## REFERENCES

- Ashley, C. C., I. P. Mulligan, and T. J. Lea. 1991.  $\text{Ca}^{2+}$  in skeletal muscle. *Q. Rev. Biophys.* 24:1–73.
- Bremel, R. D., and A. Weber. 1972. Cooperation within actin filament in vertebrate skeletal muscle. *Nature New Biol.* 238:97–101.
- Brenner, B. 1988. Effect of  $\text{Ca}^{2+}$  on cross-bridge turnover kinetics in skinned single rabbit psoas fibers: implications for regulation of muscle contraction. *Proc. Natl. Acad. Sci. USA.* 85:3265–3269.
- Brenner, B., M. Schoenberg, J. M. Chalovich, L. E. Greene, and E. Eisenberg. 1982. Evidence for crossbridge attachment in relaxed muscle at low ionic strength. *Proc. Natl. Acad. Sci. USA.* 79:7288–7291.
- Burton, B., M. Irving, and J. Sleep. 1989. The rate of force recovery after rapid shortening and restretch is equal to that after photolysis of caged ATP at  $10^\circ\text{C}$  in rabbit psoas muscle. *Biophys. J.* 55:10a. (Abstr.)
- Dantzig, J. A., M. G. Hibberd, D. R. Trentham, and Y. E. Goldman. 1991. Cross-bridge kinetics in the presence of MgADP investigated by photolysis of caged ATP in rabbit psoas muscle fibres. *J. Physiol.* 432: 639–680.
- Dawes, E. A., and J. N. Davidson. 1972. Quantitative Problems in Biochemistry, 5th ed. Churchill Livingstone, Edinburgh, UK.
- Ebashi, S., M. Endo, and I. Ohtsuki. 1969. Control of muscle contraction. *Q. Rev. Biophys.* 2:351–384.
- Fuchs, F. 1977. Cooperative interactions between calcium-binding sites on glycerinated muscle fibers: the influence of cross-bridge attachment. *Biochim. Biophys. Acta.* 462:314–322.
- Goldman, Y. E., and M. G. Hibberd. 1983.  $\text{Ca}^{2+}$ -dependence of tension transients initiated by photolysis of caged adenosine triphosphate in rabbit skinned muscle fibres. *J. Physiol.* 341:38P. (Abstr.)
- Goldman, Y. E., M. G. Hibberd, and D. R. Trentham. 1984a. Initiation of active contraction by photogeneration of adenosine-5'-triphosphate in rabbit psoas muscle fibres. *J. Physiol.* 354:605–624.
- Goldman, Y. E., M. G. Hibberd, and D. R. Trentham. 1984b. Relaxation of rabbit psoas muscle fibres from rigor by photochemical generation of adenosine-5'-triphosphate. *J. Physiol.* 354:577–604.
- Goldman, Y. E., and J. H. Kaplan. 1988. Activation of skeletal muscle fibers by photolysis of DM-nitrophen, a new caged  $\text{Ca}^{2+}$ . *Biophys. J.* 53:25a. (Abstr.)
- Griffiths, P. J., J. J. Kuhn, K. Guth, and J. C. Ruegg. 1979. Rate of isometric tension development in relation to calcium binding to skinned muscle fibres. *Pflügers Arch.* 382:165–170.
- Hibberd, M. G., J. A. Dantzig, D. R. Trentham, and Y. E. Goldman. 1985. Phosphate release and force generation in skeletal muscle fibers. *Science.* 228:1317–1319.
- Hoar, P. E., C. W. Mahoney, and W. G. L. Kerrick. 1987. MgADP increases maximum tension and  $\text{Ca}^{2+}$  sensitivity in skinned rabbit soleus fibers. *Pflügers Arch.* 410:30–36.

- Horiuti, K., T. Sakoda, M. Takei, and K. Yamada. 1992a. Effects of ethylene glycol on the kinetics of contraction on flash photolysis of caged ATP in rat psoas muscle fibres. *J. Muscle Res. Cell Motil.* 13:199–205.
- Horiuti, K., T. Sakoda, and K. Yamada. 1992b. Time course of rise of muscle stiffness at onset of contraction induced by photorelease of ATP. *J. Muscle Res. Cell Motil.* 13:685–691.
- Horiuti, K., T. Sakoda, and K. Yamada. 1993. Mechanical response to photolytic ATP pulses of skinned muscle fibres pre-activated with a small pulse of ATP. *J. Muscle Res. Cell Motil.* 14:335–340.
- Horiuti, K., N. Yagi, S. Takemori, M. Watanabe, K. Wakabayashi, and K. Yamada. 1994. Structural changes of crossbridges on contraction and relaxation induced by photolysis of caged ATP: an x-ray diffraction study at the Photon Factory. In *Synchrotron Radiation in the Biosciences*. B. Chance, J. Deisenhofer, S. Ebashi, D. T. Goodhead, J. R. Helliwell, H. E. Huxley, T. Iizuka, J. Kirz, T. Mitsui, E. Rubenstein, N. Sakabe, T. Sasaki, G. Schmahl, H. B. Stuhmann, K. Wuthrich, and G. Zaccai, editors. Oxford University Press, Oxford, UK. 486–492.
- Millar, N. C., and E. Homsher. 1990. The effect of phosphate and calcium on force generation in glycerinated rabbit skeletal muscle fibers. *J. Biol. Chem.* 265:20234–20240.
- Moiescu, D. G. 1976. Kinetics of reaction in calcium-activated skinned muscle fibres. *Nature.* 262:610–613.
- Rueben, J. P., P. W. Brandt, M. Berman, and H. Grundfest. 1971. Regulation of tension in the skinned crayfish muscle fiber. I. Contraction and relaxation in the absence of Ca ( $pCa > 9$ ). *J. Gen. Physiol.* 57:385–407.
- Sakoda, T., and K. Horiuti. 1992. Effects of ethylene glycol and calcium on the kinetics of contraction induced by photo-release of low concentrations of ATP in rat psoas muscle fibres. *J. Muscle Res. Cell Motil.* 13:464–472.
- Thirlwell, H., F. Bancel, and M. A. Ferenczi. 1993. Relaxation of rigor tension by photolysis of caged-ATP in permeabilised fibres of the rabbit. *Biophys. J.* 64:251a. (Abstr.)
- Walker, J. W., Z. Lu, and R. L. Moss. 1992. Effects of  $Ca^{2+}$  on the kinetics of phosphate release in skeletal muscle. *J. Biol. Chem.* 267:2459–2466.
- Walker, J. W., and R. L. Moss. 1990. Effects of  $Ca^{2+}$  on cross-bridge transitions measured by photo-generation of Pi and ATP. *Biophys. J.* 57:538a. (Abstr.)